Making 1H-1H couplings more accessible and accurate with selective 2DJ NMR experiments aided by 13C satellites

François-Xavier Cantrelle, Emmanuelle Boll, Davy Sinnaeve

Making ^{1}H-^{1}H couplings more accessible and accurate with selective 2DJ NMR experiments aided by ^{13}C satellites

François-Xavier Cantrelle,[1,2] Emmanuelle Boll[1,2] and Davy Sinnaeve[1,2]*

[1] CNRS, EMR9002 - Integrative Structural Biology, F-59000 Lille, France.

[2] Univ. Lille, Inserm, CHU Lille, Institut Pasteur de Lille, U1167 - RID-AGE - Risk Factors and Molecular Determinants of Aging-Related Diseases, F-59000 Lille, France.

* Corresponding author: davy.sinnaeve@univ-lille.fr

ABSTRACT

^{1}H-^{1}H coupling constants are one of the primary sources of information for NMR structural analysis. Several selective 2DJ experiments have been proposed that allow their individual measurement at pure shift resolution. However, all these experiments fail in the not uncommon case when coupled protons have very close chemical shifts. Firstly, the coupling between protons with overlapping multiplets is inaccessible due to the inability of a frequency-selective pulse to invert just one of them. Secondly, the strong coupling condition affects the accuracy of coupling measurements involving third spins. These shortcomings impose a limit on the effectiveness of state-of-the-art experiments, such as G-SERF or PSYCHEDELIC. Here, we introduce two new and complementary selective 2DJ experiments that we coin SERFBIRD and SATASERF. These experiments overcome the aforementioned issues by utilizing the ^{13}C satellite signals at natural isotope abundance, which resolve the chemical shift degeneracy. We demonstrate the utility of these experiments on the tetrasaccharide stachyose and the challenging case of norcamphor, for the latter achieving measurement of all J_{HH} couplings while only few were accessible with PSYCHEDELIC. The new experiments are applicable to any organic compound and will prove valuable for configurational and conformational analyses.

INTRODUCTION

Accurate knowledge of NMR coupling constants is of prime importance for molecular structure analysis.[1] Vicinal scalar couplings deliver direct information on dihedral angles between protons and are thus sensitive to molecular configuration and conformation. For natural product structure elucidation, all scalar couplings can be confronted with density functional theory calculations to validate a structure proposal.[2] Also residual dipolar couplings (RDCs) provide a valuable supplement for configurational analysis.[3] Homonuclear ^{1}H-^{1}H couplings are particularly valuable in this respect given their abundance in organic molecules and the sensitivity of ^{1}H NMR, but this abundance also hampers their quantification. Individual ^{1}H-^{1}H couplings are often not straightforward to extract from complex multiplets, especially if they overlap. Stefan Berger proposed an elegant solution to this problem with the SERF experiment, in which frequency-selective pulses are combined with a 2D J-resolved (2DJ) experiment in such a way that only couplings to a chosen proton appear along the indirect dimension.[4] Many further improvements have been proposed,[5] including the simultaneous observation of the full spectral bandwidth by employing the

Zangger-Sterk[6] or PSYCHE[7] elements, yielding the G-SERF and PSYCHEDELIC experiments, respectively.[8] Selective 2DJ experiments are closely related to pure shift NMR,[5b,9] and both are easily combined to homodecouple the chemical shift dimension, greatly improving spectral resolution.[8b,10] This has allowed extraction of individual couplings even for complex molecules or mixtures featuring very crowded ^{1}H NMR spectra.[5a,11]

Despite these advances, all current selective 2DJ methods suffer from one major and fundamental limitation. When two coupled protons have close chemical shifts, meaning their difference in resonance frequencies approaches the value of the coupling, the first order approximation of the nuclear spin Hamiltonian is no longer valid. This situation is referred to as strong coupling, and affects the multiplet structures in a complex way. This includes perturbations in both line intensities (*cf.* the well-known roof-effect) and line positions within the multiplet. For a simple ABX spin system, where A and B are the strongly coupled protons and X a proton weakly coupled to both A and B, theoretical analyses reveal that the line splittings associated with J_{AX} and J_{BX} are no longer exactly equal to those couplings.[12] This thus affects the accuracy of the coupling measurement. In principle this could be compensated for with spin-simulations, but in practice this is complicated for more complex spin systems and requires knowledge of all chemicals shifts and J-couplings involved. Within 2DJ spectroscopy and pure shift NMR spectra, strong coupling also leads to unwanted additional responses, commonly referred to as strong coupling 'artifacts' (even though these are not caused by an instrumental imperfection, but an inherent response from the spin system on the experiment).[13] For selective 2DJ spectroscopy, an additional complication arises. When strongly coupled protons are nearly or fully chemical shift degenerate, their multiplets typically will overlap and the individual lines within them cannot be 'purely' associated with one proton. The spin-states of these protons thus cannot be independently inverted using a frequency-selective pulse, and the coupling between them is inaccessible with current selective 2DJ methods.

Especially for compounds where protons of the same spin system tend to fall in a narrow chemical shift range, such as carbohydrates or aliphatic compounds, strong coupling situations are often encountered, even at high magnetic field strengths. Here, we introduce two selective 2DJ experiments that circumvent the strong coupling situation by focusing on the ^{13}C satellite signals at natural isotope abundance. The first experiment uses the BIRD pulse sequence element[14] to achieve active spin refocusing, and therefore is coined SERFBIRD (SElective ReFocusing using BIRD). The second experiment, named SATASERF (^{13}C SATellite Aided SElective ReFocusing), works in a similar way, but uses a bandselective pulse instead of BIRD. Whereas SERFBIRD is the most sensitive of the two experiments, its use is restricted to observing protons that are part of methine fragments. SATASERF does not have this constraint, though compromises on sensitivity and time-efficiency. Both experiments are thus complementary. The experiments will first be illustrated on the simple case of pyridine, and next on the challenging cases of the tetrasaccharide stachyose and the organic compound norcamphor for which several ^{1}H-^{1}H couplings could not be extracted using SERF, G-SERF or PSYCHEDELIC experiments.

RESULTS

Proof of principle. The phenomenon where ^{13}C-isotopomers at natural abundance overcomes the complications from strong coupling between protons bound to different carbons was first reported over 60 years ago.[15] Figure 1a shows a simulation of an ABX ^{1}H

spin system with all protons bound to ^{12}C nuclei. H_A and H_B are strongly coupled with a difference in frequency $\Delta\nu_{12C} = \nu_B - \nu_A$ of 16 Hz and a coupling J_{HAHB} of 12 Hz, while H_X is weakly coupled to H_A and H_B. The near-degeneracy of H_A and H_B causes their multiplets to coalesce, and a frequency selective pulse would not be able to invert 'purely' the H_A or H_B spins. Moreover, the H_A-H_X and H_B-H_X splittings observed on the H_A and H_B multiplets (and on the H_X multiplet, not shown) are found to be ca. 8.5 Hz and 4.5 Hz, whereas the input J_{AX} and J_{BX} couplings in the simulation were 9.0 and 4.0 Hz. 2DJ spectra would display similar discrepancies between line splittings and J-couplings.[12] Figures 1b and 1c illustrate how the presence of a single ^{13}C nucleus bound to either H_A or H_B fully overcomes all these complications by introducing a $^1J_{CH}$ coupling (145 Hz). At natural ^{13}C isotope abundance (1.1%), it is safe to neglect responses from isotopomers featuring a second ^{13}C nucleus at a specific position. For simplicity, the simulation ignores small $^2J_{CH}$ couplings and ^{13}C isotope shifts. Since the ^{13}C-bound proton's multiplet shifts either left or right depending on the ^{13}C spin isomer (α or β), and the ^{12}C-bound proton stays put, the effective frequency difference between H_A and H_B increases significantly compared to the *all*-^{12}C isotopomer. For the $^{13}C_A$ isotopomer, these become $\Delta\nu_{13CA\alpha} = \Delta\nu_{12C} - {}^1J_{CAHA}/2$ and $\Delta\nu_{13CA\beta} = \Delta\nu_{12C} + {}^1J_{CAHA}/2$ for $H_A[^{13}C^{\alpha}]$ and $H_A[^{13}C^{\beta}]$, respectively. The strong coupling situation is nearly fully lifted, with cleanly separated H_A and H_B multiplets and near-first order multiplet structures, except for a remaining modest roof effect. Importantly, the observed A-X and B-X splittings on these ^{13}C satellites are now identical to the actual J_{AX} and J_{BX} couplings within 0.05 Hz precision. This illustrates that ^1H-^1H coupling measurements in many cases should benefit from focusing on ^{13}C satellite signals.

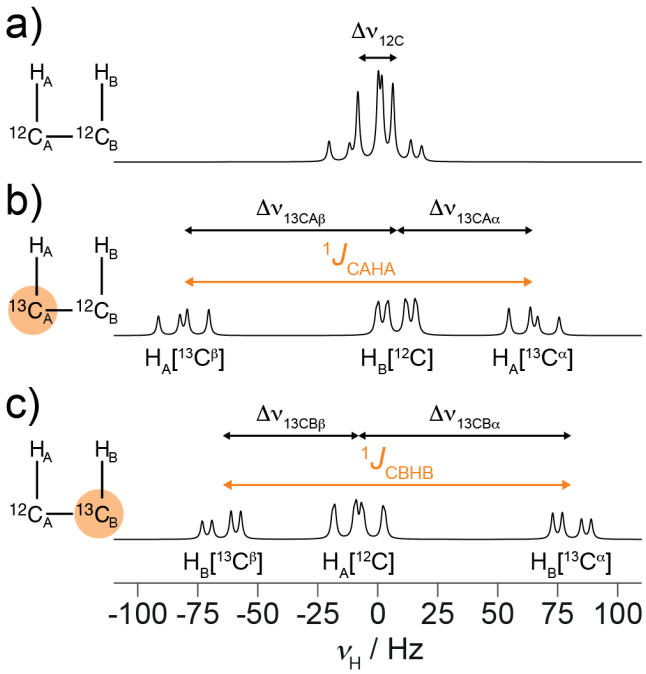

Figure 1. (a) Simulated 1D ^1H spectrum, showing the AB part of an ABX proton spin system (ν_A = –8.0 Hz, ν_B = 8.0 Hz, ν_X = 800.0 Hz, J_{AB} = 12.0 Hz, J_{AX} = 9.0 Hz, J_{BX} = 4.0 Hz). (b) Same as (a), but adding in a $^{13}C_A$ spin with $^1J_{CAHA}$ = 145 Hz and $^2J_{CAHB}$ = 0 Hz. (c) Same as (a), but adding in a $^{13}C_B$ spin with $^2J_{CBHA}$ = 0 Hz and $^1J_{CBHB}$ = 145 Hz.

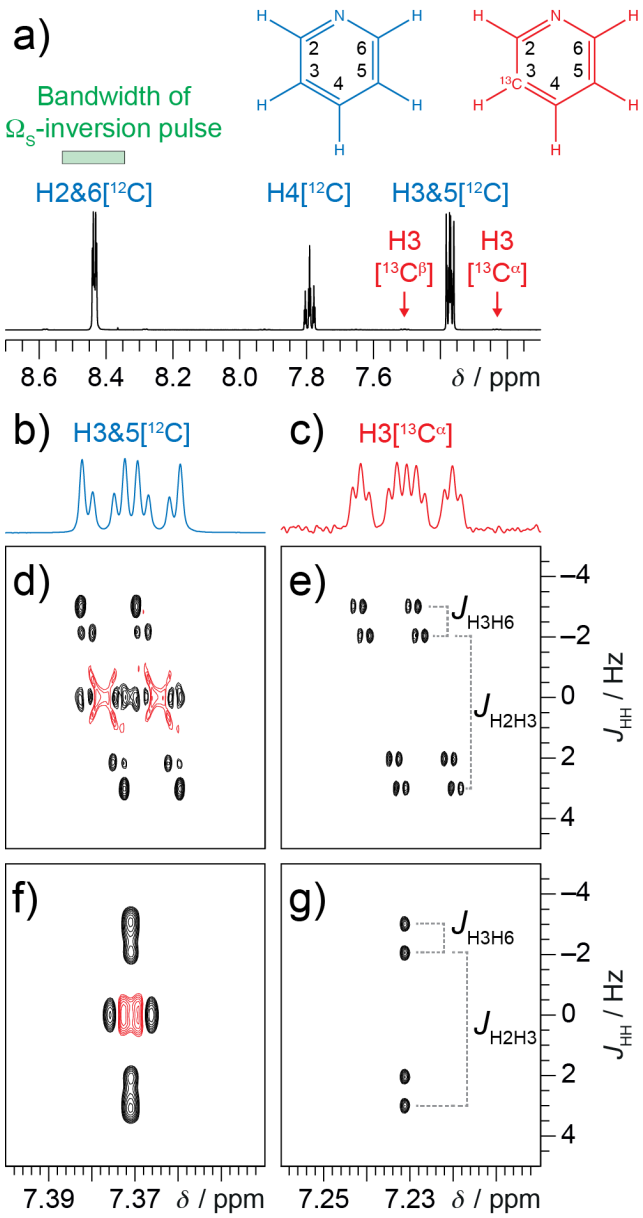

Figure 2. (a) 1D ^{1}H spectrum of pyridine, indicating the inversion bandwidth of the Ω_S-selective pulse and the H3 ^{13}C satellites. The multiplet structures of H3&5[^{12}C] and H3[^{13}C$^{\beta}$] are compared in (b) and (c), respectively. (d) Non-pure shifted TSE-PSYCHEDELIC spectrum showing the H2&H3[^{12}C] multiplet, with the Ω_S-selective pulse set to H2&6[^{12}C]. (e) Non-pure shift SERFBIRD spectrum, showing the H3[^{13}C$^{\alpha}$] satellite with the Ω_S-selective pulse set to H2&6[^{12}C]. (f) Same as (d), but with interferogram pure shift acquisition (note the digital resolution in F_1 is lower than in (d) for time-saving reasons). (g) Same as (e), but with real-time BIRD pure shift acquisition.

Figure 2 shows a real demonstration on pyridine. In the *all*-^{12}C isotopomer, the protons H3 and H5 are chemically equivalent ($\Delta\nu_{12C} = 0$), and since a small $^{4}J_{H3H5}$ coupling exists (1.4 Hz), they are infinitely strongly coupled. Because the couplings from any other proton to H3 and H5 are different, this represents a textbook example of magnetic inequivalence, yielding a second order multiplet (Figure 2b). In the $^{13}C_3$ isotopomer, this chemical shift degeneracy is broken, with $|\Delta\nu_{13C3\alpha}| = |\Delta\nu_{13C3\beta}| = 82$ Hz. As this is much larger than $^{4}J_{H3H5}$, the ^{13}C satellites display a first order multiplet (Figure 2c). Figures 2d-e compares TSE-PSYCHEDELIC[16] with the new SERFBIRD experiment, where in each case the chemically equivalent protons H2 and H6 are inverted by a Ω_S-selective 180° pulse so that only

couplings to these protons feature in F_1. TSE-PSYCHEDELIC delivers a complicated 2DJ spectrum for the H3&H5[^{12}C] multiplet, with peak intensity distortions and intense strong coupling artifacts that also feature phase-twisted line shapes. The line splittings only very slightly deviate from the actual $^3J_{H2H3}$ and $^5J_{H3H6}$ couplings in this example due to the small value of $^4J_{H3H5}$. In contrast, SERFBIRD focuses on the H3[^{13}C$^{\alpha}$] satellite signal, which delivers a 2DJ spectrum showing clean doublet of doublets, void from unwanted signals and with full absorption mode line shapes, from which the $^3J_{H2H3}$ and $^5J_{H3H6}$ couplings are straightforwardly read in F_1. Pure shift versions of TSE-PSYCHEDELIC and SERFBIRD are shown in Figures 2f and 2g, which remove all remaining couplings from the chemical shift F_2 dimension.

Since the $^1J_{C3H3}$ coupling breaks the frequency degeneracy of H3 and H5, the ^{12}C-bound H5 proton can be inverted separately from H3 using the Ω_S-selective 180° pulse (Figure 3a). The resulting pure shifted SERFBIRD experiment is shown in Figure 3b, revealing the $^4J_{H3H5}$ coupling. This coupling is not accessible from SERF, G-SERF or PSYCHEDELIC experiments that focus on the *all*-^{12}C isotopomer signals.

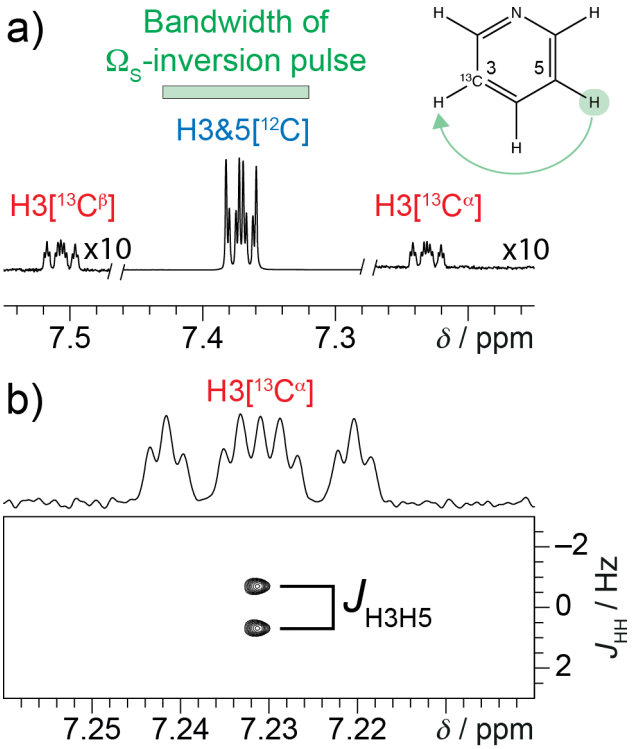

Figure 3. (a) Part of the 1D ^{1}H spectrum of pyridine showing the H3&5[^{12}C] multiplet and the H3 ^{13}C satellites. (b) Pure shifted SERFBIRD spectrum observing H3[^{13}C$^{\alpha}$] and with the inversion bandwidth of the Ω_S-selective pulse set as indicated in (a).

Pulse sequences. The SERFBIRD and SATASERF sequences are shown in Figure 4. Each first apply a ^{13}C-isotopomer filter, whose primary purpose is to suppress the ^{12}C-bound ^{1}H signals via pulse field gradient (PFG) enforced coherence transfer pathway selection, followed by a selective 2DJ sequence with optional pure shift acquisition.

SERFBIRD (Figure 4a) uses an INEPT-ST2PT sequence as ^{13}C-isotopomer filter. The single transition to single transition polarization transfer (ST2PT)[17] delivers either the ^{13}C$^{\alpha}$ or ^{13}C$^{\beta}$ satellite in one scan, avoiding a doubling of responses relative to the regular ^{1}H spectrum. It also provides optimal sensitivity by applying the principle of sensitivity improvement[18] and

by using both the ^{1}H and ^{13}C steady-state polarizations.[17] As SERFBIRD does not tolerate geminal ^{1}H-^{1}H couplings (*vide infra*), the ^{13}C to ^{1}H polarization transfer is optimized for methine (^{13}CH) groups only. Optionally, residual signals from methylene protons ($^{13}CH_2$) can be suppressed further using difference spectroscopy by alternating the Δ_a and Δ_b delays between transients. It is also possible to co-sample ^{13}C chemical shift evolution with a weighting factor *k* relative to the J_{HH} sampling in a similar way as in the $^{2}J_{HH}$-resolved HSQC by Parella and coworkers (*vide infra*).[19] Alternatively, a ^{13}C selective pulse can be used for spectral editing (see supporting information). The selective 2DJ part of SERFBIRD follows the general scheme proposed for such experiments.[5b] At natural isotope abundance, the central BIRD element ensures active spin refocusing for the observed protons experiencing a $^{1}J_{CH}$ coupling, except if they experience a geminal ^{1}H-^{1}H coupling.[14a] Its combination with the two frequency-selective 180° inversion pulses set to a chosen proton *S* at offset Ω_S ensures only a net evolution during t_1 of ^{1}H-^{1}H couplings involving this proton. Double absorption mode line shapes are obtained using the Pell-Keeler method and making good use of the frequency selective pulses.[8b,16,20] For this, experiments with normal (N) and reversed (R) sense coupling evolution are recorded by alternating the positions of the t_1 evolution periods in the sequence. When co-sampling ^{13}C chemical shift evolution, this is done in conjunction with echo/anti-echo encoding.[21] To increase sensitivity and spectral resolution in F_2, real-time BIRD pure shift acquisition can be used.[22] The homonuclear decoupling scheme is similar to the one used by Kiraly *et al.*,[22b] except that no ^{13}C composite pulse decoupling is applied, preserving the spin-state of the ^{13}C nucleus. This also avoids sample heating, allowing for longer acquisition times and higher digital resolution along F_2. Alternatively, interferogram pure shift acquisition is possible which under specific circumstances may be preferred (see supporting information). The combination of 2DJ and pure shift acquisitions have been shown to lead to enhanced chunking artifacts that are anti-phase in F_1.[23] Except when ^{13}C chemical shift is co-sampled in t_1, this can be mitigated thanks to the Pell-Keeler method since symmetric spectra along F_1 are expected.[16,24]

The SATASERF pulse sequence (Figure 4b) is similar to SERFBIRD, but with two main differences. Firstly, a frequency selective 180° pulse set to a particular ^{13}C satellite of the observed proton at offset Ω_I is used instead of BIRD, just as in SERF. Secondly, instead of ST2PT, ^{13}C anti-phase magnetization is simply converted to ^{1}H anti-phase magnetization without refocusing it to in-phase magnetization. This is because SATASERF's main use is the observation of protons from $^{13}CH_2$ groups, and sensitivity improvement and ^{13}C spin-state selective excitation schemes work far less well in such cases. This does make SATASERF inherently less sensitive than SERFBIRD (see Figure S1). Retaining the anti-phase mode of the ^{1}H-^{13}C doublet avoids complications with J_{CH} phase-modulations, while generating both ^{13}C satellites is not an issue given the Ω_I-selective 180° pulse usually already selects for just one of them. When using pure shift acquisition, typically the interferogram approach will be preferred in this case (see supporting information).[9]

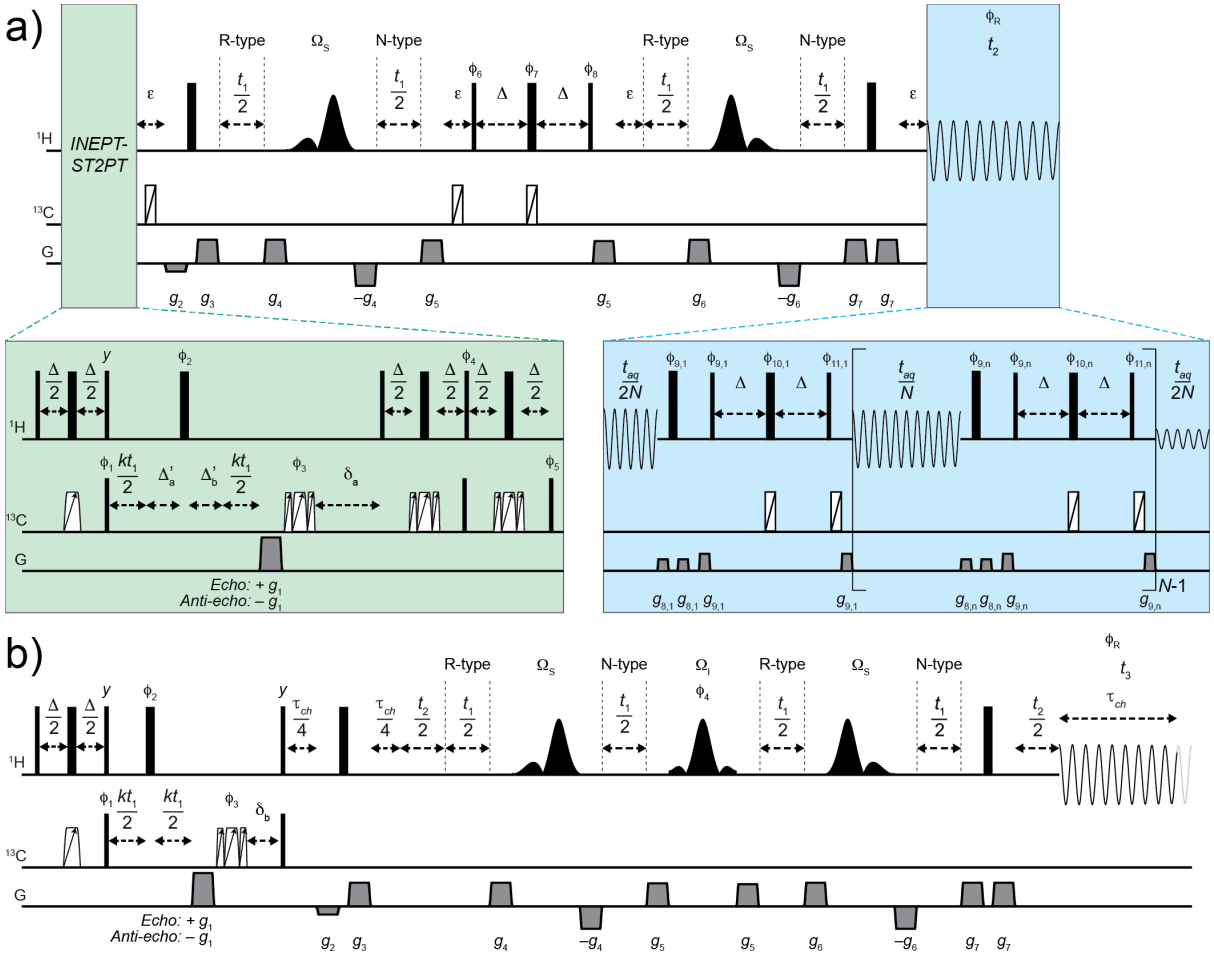

Figure 4. (a) SERFBIRD pulse sequence featuring real-time BIRD pure shift acquisition (blue box) and an INEPT-ST2PT scheme for ^{13}C isotopomer filtration and ^{13}C spin isomer selection (green box). (b) SATASERF pulse sequence, here shown with interferogram pure shift acquisition. Narrow and thick black rectangles are hard 90° and 180° pulses, respectively. Asymmetrical and symmetrical bell-shaped pulses are Ω_S-inversion and Ω_I-refocusing 180° selective pulses, respectively. Trapezoids with arrows are frequency-swept 180° pulses. White rectangles with diagonal line are Broadband Inversion Pulses (BIP) of duration ε.[25] Grey trapezoids are PFGs. The delay Δ equals $(2\times{}^1J_{CH})^{-1}$. If CH_2 signal suppression is used, $\Delta_a = 0$ and $\Delta_b = (2\times{}^1J_{CH})^{-1}$ in every odd transient and $\Delta_a = 0$ and $\Delta_b = (2\times{}^1J_{CH})^{-1}$ in every even transient, and if not, $\Delta_a = \Delta_b = 0$. The delays δ_a and δ_b serve to refocus ^{13}C chemical shift (except for kt_1) and $^1J_{CH}$ coupling evolution. For real-time pure shift acquisition, t_{aq} is the total acquisition time and N is the number of data chunks. For interferogram acquisition, τ_{ch} is the duration of the chunk of time domain data. Echo/anti-echo processing is performed using two separate datasets that either use the N-type t_1 delays and $+g_1$ gradient, or the R-type t_1 delays and $-g_1$ gradient. PFG amplitudes and phase cycles are listed in Tables S1-S3. In SERFBIRD, the phase ϕ_5 controls the choice of ^{13}C satellite.

Demonstration on stachyose

NMR spectral analysis of saccharides is often hampered by the narrow range of ^1H chemical shifts, resulting in substantial multiplet overlap and rampant strong coupling situations.[1a] We chose the tetrasaccharide stachyose (Gal1(α1→6)Gal2(α1→6)Glc3(α1→2β)Fru4) as a representative example.[26] Within the *all*-^{12}C isotopomer, the H2[^{12}C] and H3[^{12}C] protons of the Gal1 unit are strongly coupled ($\Delta\nu_{12C}$ = ca. 18 Hz, $^3J_{H2H3}$ = 10.3 Hz). Their multiplets also overlap, as is the most easily observed from the ^{13}C-decoupled HSQC spectrum (Figure 5a), making it impossible to invert just one of them using a Ω_s-selective pulse in SERF or PSYCHEDELIC experiments. Within the $^{13}C_2$ or $^{13}C_3$ isotopomers, the H2[$^{13}C^{\alpha}$] and H3[$^{13}C^{\alpha}$] signals are sufficiently shifted away from H3[^{12}C] ($\Delta\nu_{13C2\alpha}$ = ca. 90 Hz) and H2[^{12}C]

($\Delta\nu_{13C3\alpha}$ = ca. 65 Hz), respectively, alleviating strong coupling and multiplet overlap, as illustrated with the aid of a non-^{13}C decoupled CLIP-HSQC[27] (Figure 5b). The $^{13}C^{\beta}$ satellites also disentangle the H2 and H3 multiplets, but the H3[$^{13}C^{\beta}$] signal turns out strongly coupled with H4[^{12}C] (not shown). The SERFBIRD experiment in Figure 5c therefore selects for the $^{13}C^{\alpha}$ spin isomers. The Ω_S-selective pulse was set to the H2[^{12}C] and H3[^{12}C] frequencies, so that the observed H2[$^{13}C^{\alpha}$] and H3[$^{13}C^{\alpha}$] responses reveal the $^3J_{H2H3}$ coupling in the F_1 dimension. Thanks to the real-time BIRD pure shift resolution, all responses are resolved along F_2.

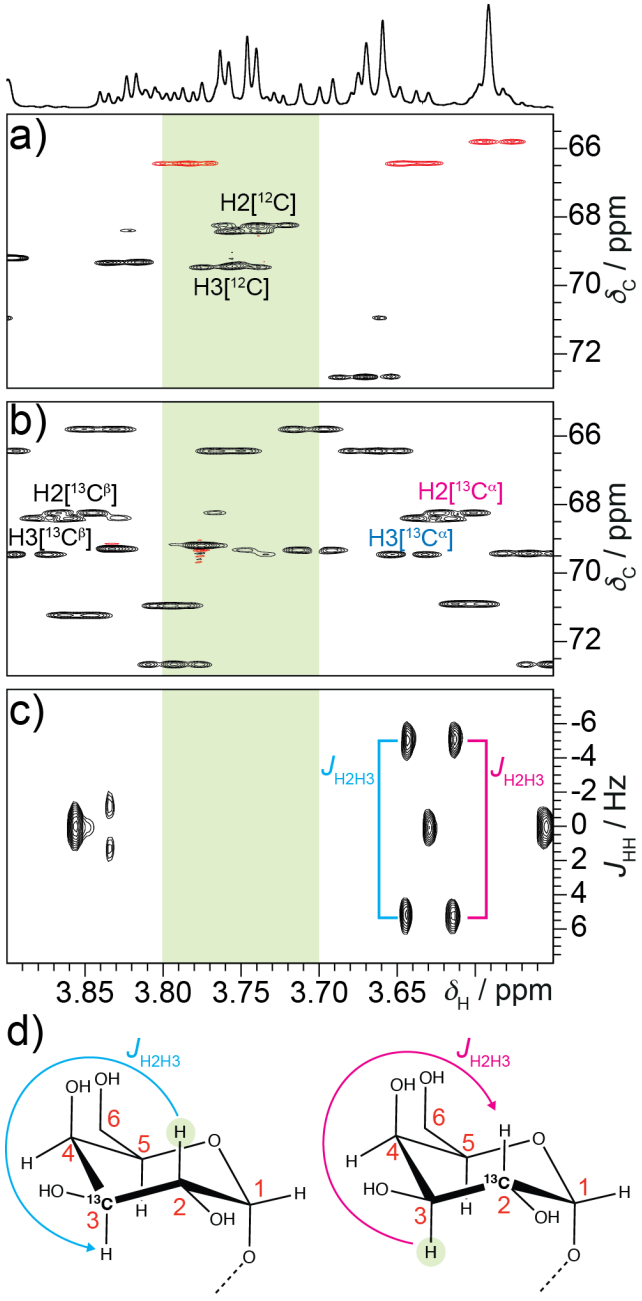

Figure 5. (a) Part of a multiplicity edited ^{1}H-^{13}C HSQC with ^{13}C-decoupling of stachyose, illustrating the overlap of the strongly coupled H2 and H3 protons in Gal1 in the absence of ^{1}H-^{13}C splittings. (b) Non-^{13}C decoupled ^{1}H-^{13}C CLIP-HSQC, revealing the positions of the ^{13}C satellites of the Gal1 H2 and H3 protons. (c) Pure shifted SERFBIRD experiment selecting for the $^{13}C^{\alpha}$ spin isomer, with the Ω_S-selective pulse set to the region highlighted in green and encompassing the H2[^{12}C] and H3[^{12}C] multiplets. (d) Structures of the observed ^{13}C isotopomers of Gal1 that facilitate the measurement of the J_{H2H3} coupling.

The strong coupling between H2[^{12}C] and H3[^{12}C] in Gal1 also affects the accuracy of coupling measurements to other protons. This is illustrated by comparing the $^{3}J_{H1H2}$ measurement in Gal1 and Gal2. In contrast to Gal1, H2[^{12}C] and H3[^{12}C] in Gal2 are better separated ($\Delta\nu_{12C}$ = ca. 45 Hz). Figure 6a shows a pure shifted TSE-PSYCHEDELIC experiment with the Ω_s-frequency selective pulse set to the anomeric H1[^{12}C] protons of both Gal1 and Gal2 in order to measure $^{3}J_{H1H2}$ on the H2[^{12}C] signals. The two obtained splittings differ by a small yet significant amount of 0.3 Hz. When ignorant of the effects of strong coupling, one may be deceived and conclude a small difference in ring conformation between both galactose units. The real reason is that the strong coupling between H2 and H3 in Gal1 causes the H1-H2 splitting to fall somewhere in-between the actual $^{3}J_{H1H2}$ and the $^{4}J_{H1H3}$ values (the latter being close to zero).[12] The same coupling measurement using the H2[^{13}C$^{\alpha}$] signals in SERFBIRD (Figure 6b) does so under a weak coupling condition for both galactose units, yielding accurate and identical $^{3}J_{H1H2}$ values.

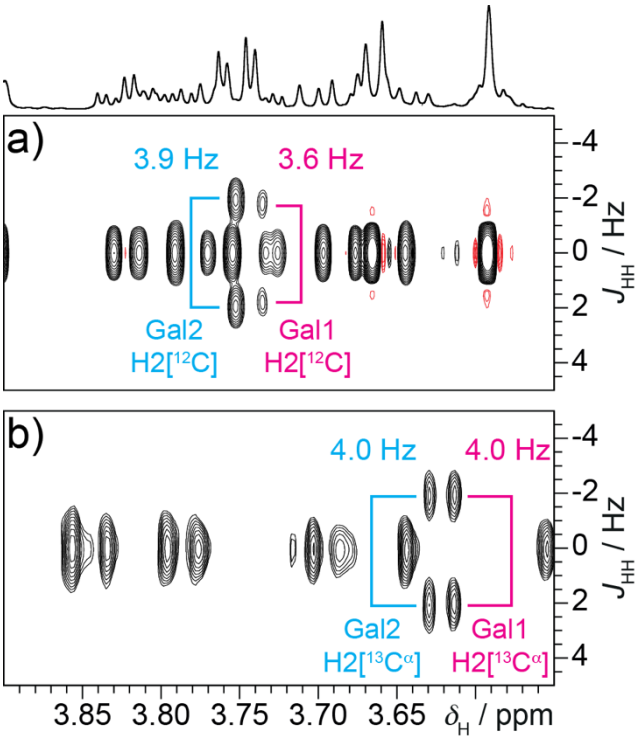

Figure 6. Pure shifted TSE-PSYCHEDELIC (a) and SERFBIRD (b) experiments on stachyose, observing the Gal1 and Gal2 H2 protons. The Ω_S-selective pulse is set to the anomeric protons in each case, and SERFBIRD selects for the $^{13}C^{\alpha}$ spin isomer.

Focusing on ^{13}C isotopomers comes with the additional advantage that we can make good use of the ^{13}C chemical shift to mitigate ^{1}H spectral overlap when even pure shift resolution turns out insufficient. An example is shown in Figure 7a, where a SERFBIRD experiment is used to measure the $^{3}J_{HH}$ coupling between the Glc3 H5 and H6b protons that are strongly coupled in the *all*-^{12}C isotopomer. Because H6b is part of a methylene group, its response is suppressed in SERFBIRD and only the H5[$^{13}C^{\beta}$] signal is visible. The H5[$^{13}C^{\beta}$] pure shift signal turns out overlapped with Fru4 H4[$^{13}C^{\beta}$], and since the Glc3 H5-H6b coupling is small, the doublet in F_1 is not cleanly resolved. Since the Glc3 $^{13}C_5$ and Fru4 $^{13}C_4$ chemical shifts are separated by 2.7 ppm (405 Hz), co-sampling a small amount (k = 0.025) of ^{13}C chemical shift evolution in t_1 provides an elegant route to disentangle these signals (Figure 7b).[19] In this

way, the two proton responses are effectively separated by ca. 10 Hz along the F_1-dimension.

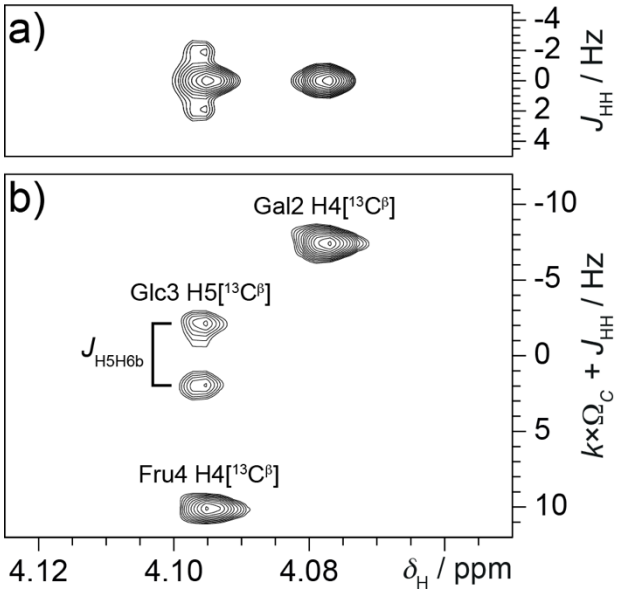

Figure 7. (a) Pure shifted SERFBIRD experiment selecting for the $^{13}C^{\beta}$ spin isomer, with the Ω_S-selective pulse set to the Glc3 H6b[^{12}C] multiplet. (b) Same as (a), but with partial co-sampling of the ^{13}C chemical shift evolution (k = 0.025).

Using SERFBIRD, nearly all vicinal ^1H-^1H couplings in stachyose could be readily extracted. The only exceptions were vicinal couplings involving the geminal proton pair H6a and H6b in Gal1, which are very strongly coupled. As both protons simultaneously experience a $^1J_{CH}$ coupling in the $^{13}C_6$ isotopomer, their strong coupling cannot be circumvented in this way. For the same reason, the geminal coupling between them could not be measured, as well as between the chemical shift degenerate Fru4 H1a-H1b protons. For measurement of the geminal Gal2 H6a-H6b and Fru4 H6a-H6b couplings, the chemical shifts of both protons were sufficiently different so that PSYCHEDELIC could be used. Measurement of the geminal Glc3 H6a-H6b coupling was complicated by strong coupling between H6b and H5. The H6b ^{13}C satellites can be used to avoid this, but as SERFBIRD cannot observe protons with geminal coupling partners, SATASERF had to be used instead (Figure S5). An overview of all extracted couplings is provided in the supporting information, with comparison to couplings extracted using PSYCHEDELIC where possible (Table S8).

Demonstration on norcamphor

Norcamphor is an important norbornane scaffold that is often used in organic chemistry. Its near-symmetrical structure presents an exceptionally challenging second order ^1H NMR spectrum with heavy multiplet overlap (Figure 8a).[28] The 5n and 6n protons are very strongly coupled ($\Delta\nu_{12C}$ = ca. 13 Hz, $^3J_{HH}$ = 9.1 Hz), as are their geminal partners 5x and 6x to a lesser degree ($\Delta\nu_{12C}$ = ca. 34 Hz, $^3J_{HH}$ = 12.0 Hz). Within the TSE-PSYCHE[29] 1D pure shift spectrum, this results in reduced intensities relative to the other signals and in severe strong coupling artifacts close to the 5n and 6n signals (Figure 8b). Given the additional heavy multiplet overlap in the ^1H spectrum, it is near-impossible to individually invert any of these four protons. This makes the majority of ^1H-^1H couplings in this small molecule inaccessible with PSYCHEDELIC or (G-)SERF experiments. Marshall and Walter previously achieved full J-coupling tabulation of norcamphor, but had to resort to syntheses of various selectively deuterated forms and spectral simulations.[28]

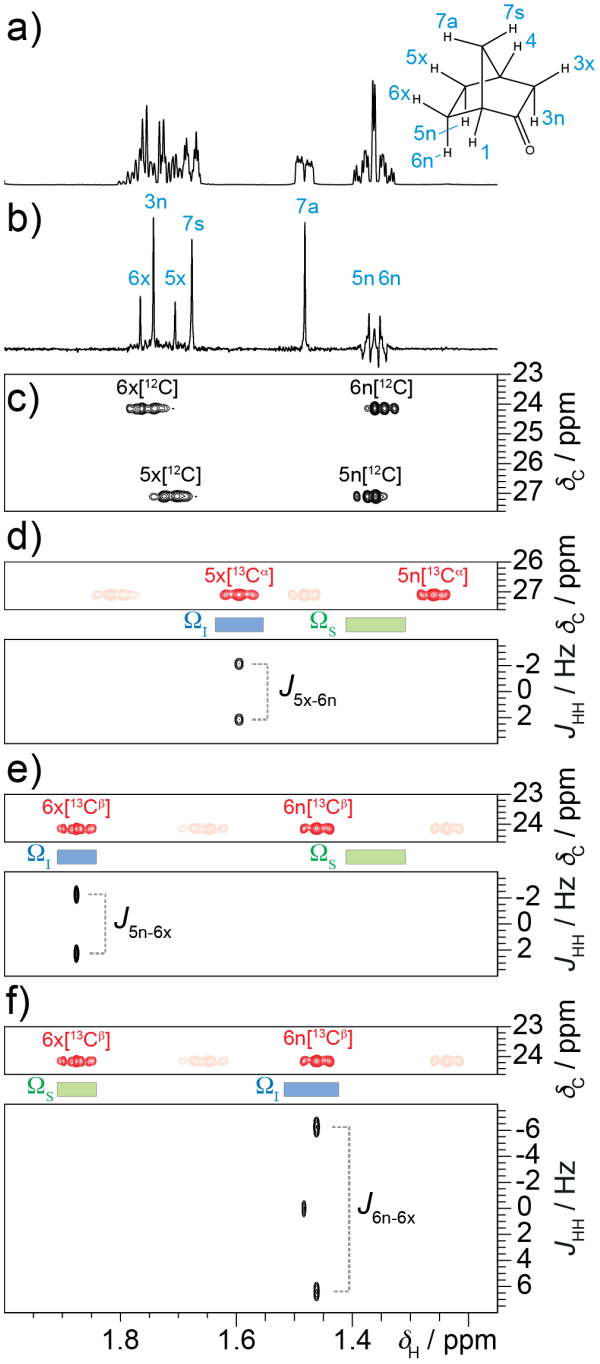

Figure 8. (a) Part of a 1D ^{1}H spectrum and structure of norcamphor. (b) 1D TSE-PSYCHE spectrum.[29] (c) Part of a ^{1}H-^{13}C HSQC with ^{13}C decoupling illustrating the multiplet positions of the 5 and 6 protons in the absence of $^{1}J_{CH}$ splittings. (d) Part of a CLIP-HSQC experiment revealing the positions of the 5x and 5n ^{13}C satellites, with the ^{13}C$^{\alpha}$ satellites highlighted, and a pure shifted SATASERF experiment with the Ω_I- and Ω_S-selective pulses set to the regions indicated. (e) and (f) are similar as (d), but highlighting the 6x and 6n ^{13}C$^{\beta}$ satellites and the Ω_I- and Ω_S-selective pulses set to different regions.

Whereas the ^{1}H spectrum of the *all*-^{12}C isotopomer is complicated, within the $^{13}C_5$ and $^{13}C_6$ isotopomers at least one ^{13}C spin isomer circumvents all strong coupling complications. The ^{13}C-decoupled HSQC in Figure 8c reveals the ^{12}C-bound frequencies, while the CLIP-HSQC in Figure 8d highlights the 5n[^{13}C$^{\alpha}$] and 5x[^{13}C$^{\alpha}$] satellites. From these, it can be seen that 5n[^{13}C$^{\alpha}$] and 5x[^{13}C$^{\alpha}$] are nicely resolved from the 6n[^{12}C] and 6x[^{12}C] multiplets, respectively. As all protons in the crowded region have geminal coupling partners, SATASERF

has to be used. The experiment in Figure 8d sets the Ω_I-selective pulse to 5x[$^{13}C^{\alpha}$] for observation, while the Ω_S-selective pulse is set to 6n[^{12}C], straightforwardly yielding the coupling between them. Similarly, the $^{13}C^{\beta}$ satellites of both the 6x and 6n protons are well-resolved from their coupling partners, and Figure 8e shows an example where the 5n-6x coupling is measured on the H6x[$^{13}C^{\beta}$] satellite. A final example in Figure 8f shows the measurement of the geminal H6n-H6x coupling on the H6x[$^{13}C^{\beta}$] satellite. Of note is that the Ω_S-selective pulse should be set to H6n[$^{13}C^{\beta}$] rather than H6n[^{12}C] in this case, as the H6x[$^{13}C^{\beta}$] and H6n[$^{13}C^{\beta}$] signals come from the same isotopomer and ^{13}C spin isomer. Using various SATASERF experiments with judiciously chosen ^{13}C satellites, we could measure *all* couplings involving *every* proton in norcamphor without strong coupling complications. This includes verification of every conceivable long-range (*i.e.*, more than three-bond) coupling in the molecule, which is a remarkable achievement given the complexity of the *all*-^{12}C isotopomer ^{1}H spectrum. An extensive revision of Marshall's coupling table[28] is provided in the supporting information (Table S12).

DISCUSSION

Since the introduction of homodecoupled selective 2DJ experiments such as push-G-SERF and PSYCHEDELIC,[5b,8b,10] the occurrence of strong coupling has been the main limiting factor for successful individual ^{1}H-^{1}H coupling extraction. The new SERFBIRD and SATASERF experiments allow bypassing this issue in many cases by focusing on^{13}C satellite signals. If accurate coupling measurement is not possible on an *all*-^{12}C isotopomer signal, then both its ^{13}C satellites essentially offer independent opportunities for measurement that is free of strong coupling complications. The ^{13}C chemical shift can be put to further good use to resolve signal overlap in cases where pure shift resolution turns out insufficient.

The only situation where this ^{13}C satellite strategy cannot work is when the strongly coupled protons are bound to the same ^{13}C spin. This is always the case for strongly coupled geminal protons, but also for ^{13}C isotopically enriched molecules. It is also conceivable that the ^{12}C-bound proton and both its ^{13}C satellites all turn out strongly coupled, each with a separate proton. This situation should be rare, and was not encountered in this work. When it does occur, a possible solution would be to move to a different magnetic field strength, as strong coupling involving ^{13}C satellites turns out very sensitive to this (see Figure S2).

As these experiments require natural ^{13}C isotope abundance, the price to pay relative to previous selective 2DJ experiments is sensitivity. SERFBIRD partly compensates for this by making optimal use of both ^{1}H and ^{13}C thermal polarizations and by real-time BIRD homodecoupling. The latter does not only improve signal intensity by collapsing the multiplet to a singlet, but it also delivers much shorter experimental times than interferogram-based pure shift experiments. SERF or G-SERF experiments can also be combined with real-time homodecoupling,[5b,10b] but line broadening due to relaxation losses between data chunks can be significant when long selective pulses are required. In contrast, real-time ^{13}C BIRD homodecoupling usually does not lead to dramatic line broadening.[22b] When sensitivity allows and methine protons need to be observed, SERFBIRD thus could be an attractive faster alternative to PSYCHEDELIC or G-SERF even when strong coupling complications do not play. In contrast, the SATASERF experiment is less sensitive, typically delivers just one coupling per experiment, and when pure shift is needed, it will usually have to resort to the slower interferogram acquisition. The optimal strategy to measure couplings on ^{13}C satellites would be to measure on methine protons using SERFBIRD as much as

possible and switch to SATASERF only when measurements on methylene protons are unavoidable.

Two NMR experiments had already been described that use ^{13}C isotopomers to measure the coupling between chemically equivalent protons. Firstly, Luy *et al.* proposed a TOCSY-based experiment with a bandselective ^{1}H spinlock that simultaneously excites the ^{12}C-bound signal and the ^{13}C-satellites, which encodes the ^{1}H-^{1}H coupling as a signal amplitude modulation.[30] Secondly, Parella and coworkers designed the Isotope Filtered SERF (IFSERF) experiment that instead uses a single bandselective 180° pulse combined with 2DJ spectroscopy.[31] Conceptually, SATASERF can be seen as a successor to IFSERF, but with full absorption mode line shapes as a key improvement. Furthermore, the design of both the TOCSY and IFSERF experiments in practice limits their use to the measurement of couplings between the chemical shift degenerate protons, and not those involving their other coupling partners. The requirement to simultaneously irradiate the ^{12}C- and ^{13}C-bound proton partners also implies that the bandselective region covered is 2-3 times wider than what would have been needed with the individual Ω_s- and Ω_I-selective pulses in SERFBIRD and SATASERF. In practice this means that it would be much harder to avoid irradiation of nearby coupling partners in crowded regions than when using the new experiments. Adding also the benefits of pure shift resolution, SERFBIRD and SATASERF thus present a much wider scope of application than these previous methods.

CONCLUSIONS

Taken together, SERFBIRD and SATASERF are an important addition to the existing set of selective 2DJ experiments, overcoming the limitations of strong coupling in many cases without having to resort to spin simulations. The examples of stachyose and norcamphor illustrate how ^{13}C satellites can be exploited even in molecules with crowded spectral regions. Besides scalar couplings, the new experiments should be applicable for ^{1}H-^{1}H RDC measurements. We envision both experiments will become valuable tools for structure analysis of any organic compound, for instance the constitution or configurational elucidation of natural products or conformational characterization of pharmaceuticals and peptides. Given its speed and sensitivity, especially SERFBIRD will be an attractive experiment for saccharides or compounds rich in alkene or aromatic groups.

SUPPORTING INFORMATION

Supporting Information

The Supporting Information contains the experimental section, phase cycles and gradient amplitudes, signal-to-noise comparisons, setup guidelines for SERFBIRD and SATASERF, simulations on the impact of magnetic field strength on strong coupling involving ^{13}C satellites, overview of NMR spectra and coupling data for stachyose and norcamphor, and the Bruker pulse sequence codes for SERFBIRD and SATASERF. NMR data can be downloaded from: http://dx.doi.org/10.5281/zenodo.10473716.

AUTHOR CONTRIBUTIONS

D.S. designed the experiments, acquired the data, and wrote the manuscript. F.-X.C. and E.M. performed sample preparation and processed the data. All authors have given approval to the final version of the manuscript.

ACKNOWLEDGEMENTS

D.S. acknowledges funding from the Agence Nationale de la Recherche (ANR) (ANR-20-CE29-0015-01 URANUS). The 600 MHz NMR spectrometer is funded by the Nord Region Council, CNRS, Institut Pasteur de Lille, the European Community (ERDF), the French Ministry of Research and the Université de Lille and by the CTRL CPER cofunded by the European Union with the European Regional Development Fund (ERDF), by the Hauts-de-France Regional Council (contract n°17003781), Métropole Européenne de Lille (contract n°2016_ESR_05), and French State (contract n°2017-R3-CTRL-Phase1). *This work is dedicated to Prof. Stefan Berger, inventor of the prototype SERF experiment,[4-5a] 1946-2023.*

REFERENCES

(1) (a) Battistel, M. D.; Azurmendi, H. F.; Yu, B.; Freedberg, D. I. *Prog. Nucl. Magn. Reson. Spectrosc.* **2014**, *79*, 48-68; (b) Thomas, W. A. *Prog. Nucl. Magn. Reson. Spectrosc.* **1997**, *30*, 183-207.
(2) (a) Gerrard, W.; Bratholm, L. A.; Packer, M.; Mulholland, A. J.; Glowacki, D. R.; Butts, C. P. *Chem. Sci.* **2020**, *11*, 508-515; (b) Koos, M. R. M.; Navarro-Vazquez, A.; Anklin, C.; Gil, R. R. *Angew. Chem. Int. Ed.* **2020**, *59*, 3938-3941.
(3) (a) Gil, R. R. *Angew. Chem. Int. Ed.* **2011**, *50*, 7222-7224; (b) Kummerlöwe, G.; Luy, B. *TrAC Trends Anal. Chem.* **2009**, *28*, 483-493; (c) Böttcher, B.; Thiele, C. M. In *eMagRes*; Wasylishen, R., Ed.; John Wiley & Sons, Ltd: Chichester, 2012; Vol. 1, pp 169-180. DOI: 10.1002/9780470034590.emrstm1194; (d) Liu, Y.; Sauri, J.; Mevers, E.; Peczuh, M. W.; Hiemstra, H.; Clardy, J.; Martin, G. E.; Williamson, R. T. *Science* **2017**, *356*, 43-+.
(4) Fäcke, T.; Berger, S. *J. Magn. Reson. Ser. A* **1995**, *113*, 114-116.
(5) (a) Berger, S. *Prog. Nucl. Magn. Reson. Spectrosc.* **2018**, *108*, 74-114; (b) Sinnaeve, D. *eMagRes* **2021**, *9*, 267-281.
(6) Zangger, K.; Sterk, H. *J. Magn. Reson.* **1997**, *124*, 486-489.
(7) Foroozandeh, M.; Adams, R. W.; Meharry, N. J.; Jeannerat, D.; Nilsson, M.; Morris, G. A. *Angew. Chem. Int. Ed.* **2014**, *53*, 6990-6992.
(8) (a) Giraud, N.; Beguin, L.; Courtieu, J.; Merlet, D. *Angew. Chem. Int. Ed.* **2010**, *49*, 3481-3484; (b) Sinnaeve, D.; Foroozandeh, M.; Nilsson, M.; Morris, G. A. *Angew. Chem. Int. Ed.* **2016**, *55*, 1090-1093.
(9) Zangger, K. *Prog. Nucl. Magn. Reson. Spectrosc.* **2015**, *86-87*, 1-20.
(10) (a) Pucheta, J. E. H.; Pitoux, D.; Grison, C. M.; Robin, S.; Merlet, D.; Aitken, D. J.; Giraud, N.; Farjon, J. *Chem. Commun.* **2015**, *51*, 7939-7942; (b) Pitoux, D.; Plainchont, B.; Merlet, D.; Hu, Z. Y.; Bonnaffe, D.; Farjon, J.; Giraud, N. *Chem. Eur. J.* **2015**, *21*, 9044-9047.
(11) (a) Pitoux, D.; Hu, Z.; Plainchont, B.; Merlet, D.; Farjon, J.; Bonnaffe, D.; Giraud, N. *Magn. Reson. Chem.* **2018**, *56*, 954-962; (b) Sinnaeve, D.; Dinclaux, M.; Cahoreau, E.; Millard, P.; Portais, J. C.; Letisse, F.; Lippens, G. *Anal. Chem.* **2018**, *90*, 4025-4031; (c) Janssen, M. A.; Thiele, C. M. *Chem. Eur. J.* **2020**, *26*, 7831-7839.
(12) (a) Kumar, A. *J. Magn. Reson.* **1978**, *30*, 227-249; (b) Bodenhausen, G.; Freeman, R.; Morris, G. A.; Turner, D. L. *J. Magn. Reson.* **1978**, *31*, 75-95.
(13) (a) Morris, G. A., "Two-Dimensional J-Resolved Spectroscopy" In *Encyclopedia of Magnetic Resonance*, eds-in-chief.; Harris, R. K., Wasylishen, R., John Wiley: Chichester. DOI: 10.1002/9780470034590.emrstm0579.pub2. Posted on-line 15th September 2009; (b) Thrippleton, M. J.; Edden, R. A. E.; Keeler, J. *J. Magn. Reson.* **2005**, *174*, 97-109.
(14) (a) Garbow, J. R.; Weitekamp, D. P.; Pines, A. *Chem. Phys. Lett.* **1982**, *93*, 504-509; (b) Aguilar, J. A.; Nilsson, M.; Morris, G. A. *Angew. Chem. Int. Ed.* **2011**, *50*, 9716-9717.

(15) Cohen, A. D.; Sheppard, N.; Turner, J. J. *Proc. Chem. Soc. Lond.* **1958**, 118-119.
(16) Sinnaeve, D.; Ilgen, J.; Di Pietro, M. E.; Primozic, J. J.; Schmidts, V.; Thiele, C. M.; Luy, B. *Angew. Chem. Int. Ed.* **2020**, *59*, 5316-5320.
(17) Pervushin, K. V.; Wider, G.; Wuthrich, K. *J. Biomol. NMR* **1998**, *12*, 345-348.
(18) Kay, L. E.; Keifer, P.; Saarinen, T. *J. Am. Chem. Soc.* **1992**, *114*, 10663-10665.
(19) Marco, N.; Nolis, P.; Gil, R. R.; Parella, T. *J. Magn. Reson.* **2017**, *282*, 18-26.
(20) Pell, A. J.; Keeler, J. *J. Magn. Reson.* **2007**, *189*, 293-299.
(21) Keeler, J.; Neuhaus, D. *J. Magn. Reson.* **1985**, *63*, 454-472.
(22) (a) Paudel, L.; Adams, R. W.; Kiraly, P.; Aguilar, J. A.; Foroozandeh, M.; Cliff, M. J.; Nilsson, M.; Sandor, P.; Waltho, J. P.; Morris, G. A. *Angew. Chem. Int. Ed.* **2013**, *52*, 11616-11619; (b) Kiraly, P.; Nilsson, M.; Morris, G. A. *Magn. Reson. Chem.* **2018**, *56*, 993-1005; (c) Kiraly, P.; Morris, G. A.; Liu, Q. X.; Nilsson, M. *Synlett* **2019**, *30*, 1015-1025; (d) Lupulescu, A.; Olsen, G. L.; Frydman, L. *J. Magn. Reson.* **2012**, *218*, 141-146.
(23) Kiraly, P.; Foroozandeh, M.; Nilsson, M.; Morris, G. A. *Chem. Phys. Lett.* **2017**, *683*, 398-403.
(24) Sinnaeve, D. *Magn. Reson. Chem.* **2018**, *56*, 947-953.
(25) Smith, M. A.; Hu, H.; Shaka, A. J. *J. Magn. Reson.* **2001**, *151*, 269-283.
(26) McIntyre, D. D.; Vogel, H. J. *J. Nat. Prod.* **1989**, *52*, 1008-1014.
(27) Enthart, A.; Freudenberger, J. C.; Furrer, J.; Kessler, H.; Luy, B. *J. Magn. Reson.* **2008**, *192*, 314-322.
(28) Marshall, J. L.; Walter, S. R. *J. Am. Chem. Soc.* **1974**, *96*, 6358-6362.
(29) Foroozandeh, M.; Adams, R. W.; Kiraly, P.; Nilsson, M.; Morris, G. A. *Chem. Commun.* **2015**, *51*, 15410-15413.
(30) Luy, B.; Hauser, G.; Kirschning, A.; Glaser, S. J. *Angew. Chem. Int. Ed.* **2003**, *42*, 1300-1302.
(31) Nolis, P.; Roglans, A.; Parella, T. *J. Magn. Reson.* **2005**, *173*, 305-309.